Mixed Finite Element Method for Miscible Displacement Problems in Porous Media

B.L. Darlow, SPE, Exxon Production Research Co.
R.E. Ewing, SPE, Mobil R&D Corp.
M.F. Wheeler, SPE, Rice U.

Abstract

Effective numerical simulation of many EOR problems requires very accurate approximation of the Darcy velocities of the respective fluids. In this paper we describe a new method for the accurate determination of the Darcy velocity of the total fluid in the miscible displacement of one incompressible fluid by another in a porous medium. The new mixed finite-element procedure solves for both the pressure and velocity of the total fluid simultaneously as a system of first-order partial differential equations. By solving for $u=(-k/\mu)\nabla p$ as one term, we minimize the difficulties occurring in standard methods caused by differentiation or differencing of p and multiplication by rough coefficients k/μ.

By using mixed finite elements for the pressure equation coupled in a sequential method with a finite element procedure for the concentration of the invading fluid, we are able to treat a variety of problems with variable permeabilities, different mobility ratios, and a fairly general location of injection and production wells. Mixed finite-element methods also produce minimal grid-orientation effect. Computational results on a variety of two-dimensional (2D) problems are presented.

Introduction

This paper considers the miscible displacement of one incompressible fluid by another in a horizontal reservoir $\Omega \subset R^2$ over a time period $J=[0,T]$. If p is the pressure of the total fluid with viscosity μ in a medium with permeability k, we define the Darcy velocity of the total fluid by

$$u=-\frac{k}{\mu}\nabla p. \quad \ldots\ldots\ldots\ldots\ldots\ldots\ldots\ldots\ldots\ldots (1)$$

Then, letting c denote the concentration of the invading fluid and ϕ denote the porosity of the medium, the coupled quasilinear system of partial differential equations describing the fluid flow is given by[1-3]

$$-\nabla\cdot\left(\frac{k}{\mu}\nabla p\right)\equiv \nabla\cdot u=q,\ x\epsilon\Omega,\ t\epsilon J, \quad \ldots\ldots\ldots (2)$$

and

$$\nabla\cdot(D\nabla c-uc)=\phi\frac{\partial c}{\partial t}-q\hat{c},\ x\epsilon\Omega,\ t\epsilon J. \quad \ldots\ldots\ldots (3)$$

Here $q=q(x,t)$ represents the total flow into or out of the region Ω ($q>0$ at injection wells and $q<0$ at production wells in this setting), $\hat{c}=\hat{c}(x,t)$ is equal to the value of c at a producing well and the specified inlet concentration at an injection well, and $D=D(x,u)$ is the diffusion-dispersion tensor given by[4]

$$[D_{ij}(x,u)]=\phi(x)d_m I+\frac{d_\ell}{|u|}\begin{pmatrix} u_1^2 & u_1u_2 \\ u_1u_2 & u_2^2 \end{pmatrix} +\frac{d_t}{|u|}\begin{pmatrix} u_2^2 & -u_1u_2 \\ -u_1u_2 & u_1^2 \end{pmatrix}, \quad \ldots\ldots\ldots\ldots (4)$$

where d_m, a small molecular diffusion coefficient, and d_ℓ and d_t, the magnitudes of longitudinal and transverse dispersion, are given constants. Here $|u|$ is the standard Euclidean norm of the vector u. To complete the description of the flow we augment the system (Eqs. 2 and 3) with a prescription of an initial concentration distribution of the invading fluid and no-flow conditions across the boundary, $\partial\Omega$, given by

$$c(x,0)=c_0(x),\ x\epsilon\Omega, \quad \ldots\ldots\ldots\ldots\ldots\ldots\ldots\ldots (5)$$

$$u\cdot\nu=0,\ x\epsilon\partial\Omega,\ te J, \quad \ldots\ldots\ldots\ldots\ldots\ldots\ldots\ldots (6)$$

and

$$\sum_{i,j=1}^{2} D_{ij}(x,u)\frac{\partial c}{\partial x_j}\nu_i=0,\ x\epsilon\partial\Omega,\ t\epsilon J, \quad \ldots\ldots\ldots\ldots (7)$$

where ν_i are components of the outward normal vector to $\partial\Omega$. Incompressibility requires that

$$\int_\Omega q(x,t)dx=0,\ t\epsilon J. \quad \ldots\ldots\ldots\ldots\ldots\ldots\ldots\ldots (8)$$

Eqs. 2 and 3 are coupled by the dependence of the viscosity, $\mu=\mu(c)$, on the concentration, c, and by the

0197-7520/84/0081-0501$00.25

dependence of $D=D(x,u)$ and the transport term, $\nabla \cdot uc$, explicitly on the Darcy velocity, u. Note that the pressure, p, does not appear explicitly in Eq. 3 in this incompressible setting. Therefore, the variable of interest in Eq. 2 is actually u instead of p. The emphasis of this paper is to describe a new numerical procedure for obtaining more accurate Darcy velocities in this context.

Standard finite difference or finite element procedures for solving Eq. 2 determine p as a set of cell averages, nodal values, or piecewise smooth functions. The resulting p is differenced or differentiated and then multiplied by a possibly rough function k/μ to determine the velocity u. These processes produce a rough and often inaccurate approximation of u that then reduces the accuracy of the approximation of the concentration, c. In this paper we consider the use of mixed finite-element methods to approximate these important velocities in a more accurate fashion. These methods were first proposed and analyzed in this context by Douglas *et al.*[5]

In the mixed finite-element method, we solve Eq. 2 for both pressure and velocity simultaneously as a system of first-order partial differential equations. By solving for $-(k/\mu)\nabla p$ as one term, we minimize the difficulties caused by rough coefficients k/μ in standard methods. We then couple our approximate solution of Eq. 2 with a finite element method for solving Eq. 3 in a sequential timestepping procedure.

At practical levels of spatial discretization, standard Galerkin methods based on tensor products of continuous piecewise polynomial functions are subject to cusping in the neighborhood of production wells and grid-orientation effects with high mobility ratio flows ($M \geq 10$).[6] New methods were devised that used function spaces discontinuous across interelement boundaries. These methods were augmented with penalties on the continuity of both function values and normal derivatives across these boundaries.[6-9] Computations using these methods showed that grid-orientation effects were greatly diminished.[7-9] However, these penalty terms also significantly increased the computational complexity of the resulting codes. One goal of the use of mixed methods is to control cusping and grid orientation without extensive use of interior penalties. As a first step in this direction, we have coupled our newly developed mixed method codes with the interior penalty Galerkin codes of Ref. 9 and will experiment with the choice of penalties to see if the improved velocities arising from the mixed methods will eliminate the need for interior penalties in some cases.

Standard finite-difference methods for solving Eq. 2 have not proved satisfactory with normal mesh spacings because of lack of accurate velocities. Also, the versatility of the finite-element formulation allows special analytical treatment of the wells by subtracting out the singular behavior of the pressure or the velocity and solving for the remaining part from a finite-element space. This technique is described in Eqs. 27 and 33. The mixed finite-element methods presented here for solving Eq. 2 produce velocities that can be combined with either finite-element or finite-difference techniques for solving Eq. 3.

Very accurate Darcy velocities are particularly important for use in other methods for solving Eq. 3 such as those using streamtubes or flowlines and modifications of the method of characteristics. Douglas[10] has combined lower order versions of the mixed methods presented here in conjunction with finite-difference versions of a method of characteristics code to solve Eq. 3. Use of mixed finite-element methods for determining accurate velocities in more general problems also is being studied.

We have produced a versatile research code to test some of the properties of our version of mixed finite-element methods in miscible displacement simulation. Our codes, which apply to two space dimensions, allow arbitrary rectangular mesh spacing, arbitrary permeabilities, and very general placement of production and injection wells. We also can test the use of tensor product dispersion of the form in Eq. 4 as well as the use of various mobility ratios. After describing the mathematical aspects of our methods in the next section, we present the results of several computational experiments designed to test the accuracy and versatility of our methods. We then state some conclusions from the preliminary testing of our codes and methods.

Mathematical Description of the Procedure

Let

$$(v,w)=\int_{\Omega} vw\,dx,$$

$$\langle v,w\rangle=\int_{\partial\Omega} vw\,ds,$$

and

$$\|v\|^2=(v,v)$$

be the standard L^2 inner products and norm on Ω and $\partial\Omega$. Let $H(\mathrm{div};\Omega)$ be the set of vector functions $v\in[L^2(\Omega)]^2$ such that $\nabla \cdot v\in L^2(\Omega)$, and let

$$V=H(\mathrm{div};\Omega)\cap\{v\cdot\nu=0 \text{ on } \partial\Omega\}. \quad \ldots\ldots\ldots\ldots (9)$$

Let $W=L^2(\Omega)$ and $H^1=H^1(\Omega)$ be standard Sobolev spaces.

We obtain the weak solution form of Eq. 1 by multiplying by a test function, $v\in V$, and integrating the result to obtain

$$(u,v)=\left(-\frac{k}{\mu}\nabla p,v\right), \quad v\in V. \quad \ldots\ldots\ldots\ldots\ldots (10)$$

Dividing each side of Eq. 10 by k/μ, integrating the resulting right side by parts, and using the properties of $v\in V$ on $\partial\Omega$, we then obtain

$$\left(\frac{\mu}{k}u,v\right)-(p,\nabla\cdot v)=0, \quad v\in V. \quad \ldots\ldots\ldots\ldots (11)$$

We next multiply Eq. 2 by a test function, $w\in W$, and integrate the result over Ω to obtain

$$-(\nabla\cdot u,w)=(q,w), \quad w\in W. \quad \ldots\ldots\ldots\ldots\ldots (12)$$

The first-order system of Eqs. 11 and 12 constitutes our weak form of the solution pair $(u; p)$ and determines our mixed method. Combining these equations with the weak form of Eq. 3, we seek a triple $(u; p; c)$ satisfying Eqs. 11 and 12, and

$$\left(\phi\frac{\partial c}{\partial t}, z\right)+(-uc+D(u)\nabla c, \nabla z)-(q\hat{c}, z)=0,$$

$$z\epsilon H^1. \quad \ldots\ldots\ldots\ldots\ldots\ldots\ldots\ldots\ldots\ldots (13)$$

Under boundedness assumptions on the coefficients of k, μ, and ϕ and positive definiteness assumptions on the matrix D, we can define and analyze continuous- and discrete-time versions of Eqs. 11, 12, and 13. We must first define the finite dimensional subspaces of V, W, and H^1, in which we shall seek approximations for u, p, and c, respectively.

For a region S, let $C^j(S)$ be the set of all functions on S that are j times continuously differentiable (defining C^{-1} to be discontinuous functions) and let $P_m(S)$ be the set of all polynomials of degree not greater than m on S. Then for a partition $\delta=\{x_0, x_1 \ldots x_N\}$, $x_i > x_{i-1}$, we obtain

$$M_j^m(\delta)\equiv\{\psi\epsilon C^j([x_0, x_N]):\psi|_{(x_{i-1}, x_i)}\epsilon P_m,\ i=1\ldots N\}.$$

$$\ldots\ldots\ldots\ldots\ldots\ldots\ldots\ldots\ldots\ldots (14)$$

Assume that $\Omega=[a,b]\otimes[c,d]$ is a rectangle in R^2 and that δ_x and δ_y are partitions of $[a,b]$ and $[c,d]$, respectively. We now define the finite dimensional spaces as

$$M_h=M^1{}_{-1}(\delta_x^c)\otimes M^1{}_{-1}(\delta_y^c), \quad \ldots\ldots\ldots\ldots\ldots (15)$$

$$W_h=M^1{}_{-1}(\delta_x^p)\otimes M^1{}_{-1}(\delta_y^p), \quad \ldots\ldots\ldots\ldots\ldots (16)$$

$$\tilde{V}_h=\{[M^2{}_0(\delta_x^p)\otimes M^1{}_{-1}(\delta_y^p)] \times[M^1{}_{-1}(\delta_x^p)\otimes M^2{}_0(\delta_y^p)]\}, \quad \ldots\ldots\ldots\ldots\ldots (17)$$

and

$$V_h=\{v\epsilon\tilde{V}_h: v\cdot\nu=0 \text{ on } \partial\Omega\}, \quad \ldots\ldots\ldots\ldots\ldots (18)$$

where the superscripts p and c on the δ's indicate that different grid sizes h_p and h_c can be used to solve the pressure equations, Eqs. 11 and 12, and the concentration equation, Eq. 13. These spaces are special cases of those defined by Raviart and Thomas.[11] Therefore M_h and W_h are discontinuous linear functions in x tensored with discontinuous linears in y, while the x-component of V_h is composed of C^0-quadratics in x tensored with discontinuous linears in y and the y-component of V_h is composed of discontinuous linears in x tensored with C^0-quadratics in y. Note that $M_h\subset H^1$, $W_h\subset W$, $\tilde{V}_h\subset H(\text{div}; \Omega)$, and $V_h\subset V$.

The continuous-time version of our mixed finite element is then:

find $(U; P; C):J\rightarrow(V_h; W_h; M_h)$ satisfying

$$\left(\frac{\mu(C)}{k}U, v\right)-(P, \nabla\cdot v)=0, \quad v\epsilon V_h, \quad \ldots\ldots\ldots (19)$$

$$(\nabla\cdot U, w)=(q, w), \quad w\epsilon W_h, \quad \ldots\ldots\ldots\ldots\ldots (20)$$

$$\left(\phi\frac{\partial C}{\partial t}, z\right)+(^-UC+D(U)\nabla C, \nabla z)-(q\hat{C}, z)=0,$$

$$z\epsilon M_h, \quad \ldots\ldots\ldots\ldots\ldots\ldots\ldots\ldots (21)$$

and

$$(C-c_0, z)=0, \ z\epsilon M_h. \quad \ldots\ldots\ldots\ldots\ldots (22)$$

The spaces V_h, W_h, and M_h have sufficiently strong approximation properties and necessary inclusion structure that we have obtained the following result.

Theorem 1. For smoothly distributed q, we have

$$\sup_{t\epsilon J}\|c-C\|\leqslant M_1h_c^2+M_2h_p^2, \quad \ldots\ldots\ldots\ldots (23)$$

$$\sup_{t\epsilon J}\|u-U\|\leqslant M_3h_c^2+M_4h_p^2, \quad \ldots\ldots\ldots\ldots (24)$$

where M_i, $i=1\ldots 4$ depend on the smoothness of p, u, and c. The proof of Theorem 1[5] uses the analysis of Brezzi,[12] Raviart and Thomas,[11] Falk and Osborn,[13] and two of the authors.[3]

In the applications considered in this paper the sources and sinks are from injection and production wells and thus are *not* smoothly distributed. In this case the regularity of all the functions suffer and convergence can be obtained only at reduced rates. At present, in the case of logarithmic singularities at sources and sinks, analysis is complete only in the special case of unit mobility ratio. This analysis was presented in Ref. 14 for standard Galerkin methods and then extended[5] to mixed methods. The results depend on whether the tensor D contains only molecular diffusion ($d_\ell=d_t=0$) or the dispersive terms also.

Theorem 2. For point sources q, we obtain

$$\sup_{t\epsilon J}\|c-C\|\leqslant M_5h^{1-\epsilon}(\text{if } d_\ell=d_t=0), \quad \ldots\ldots (25)$$

$$\sup_{t\epsilon J}\|c-C\|\leqslant M_6h^{1/2-\epsilon}(\text{if } d_\ell\neq 0 \text{ and } d_t\neq 0), \quad \ldots (26)$$

where $\epsilon>0$ is arbitrarily small and M_5 and M_6 depend on the regularity of the unknowns.

We next consider discrete-time methods. Our methods depend on preconditioned conjugate gradient iteration for both the concentration and the pressure equations. Extensive analysis of these techniques for standard Galerkin methods is given in Ref. 15 and has been extended to the mixed method case by one of the authors. Our discrete codes also use interior penalties. Analysis of these techniques by two of the authors for the concentration equation in the miscible displacement setting has

been published.[7] A timestepping method in the mixed method context has been published also.[16]

To treat the point sources and sinks in our codes, we subtract out logarithmic singularities at the wells and solve for the remaining portion of the pressure. A particularly convenient way to do this, emphasizing the desire to obtain accurate velocities, is described in the following.

Assume that u can be represented in the form

$$u=u_s+u_r,$$

where u_s, the singular part, is given by

$$u_s=\sum_{j=1}^{N} Q_j(t)\nabla N_j,\ N_j=\frac{1}{2\pi}\log|x-x_j|, \quad \ldots\ldots(27)$$

where $Q_j(t)$ are the flow rates at the wells located at x_j, and u_r, the regular part, satisfies the relations

$$\nabla\cdot u_r=0,\ x\epsilon\Omega, \quad \ldots\ldots(28)$$

and

$$u_r\cdot\nu=-u_s\cdot\nu,\ x\epsilon\partial\Omega, \quad \ldots\ldots(29)$$

for $t\epsilon J$. The pressure equations, 19 and 20, then can be replaced by

$$\left(\frac{\mu(C)}{k}U_r,v\right)-(\nabla\cdot v,P)=-\left(\frac{\mu(C)}{k}u_s,v\right),\ v\epsilon V_h, \quad \ldots\ldots(30)$$

$$(\nabla\cdot U_r,w)=0,\ w\epsilon W_h, \quad \ldots\ldots(31)$$

and

$$\langle(U_r+u_s)\cdot\nu,\ v\cdot\nu\rangle=0,\ v\epsilon\tilde{V}_h, \quad \ldots\ldots(32)$$

where now $U_r\epsilon\tilde{V}_h$ instead of V_h. Eq. 32 requires that the net flow across $\partial\Omega$ of each boundary element be zero. Then set

$$U=U_r+u_s. \quad \ldots\ldots(33)$$

The algebraic system arising from Eqs. 30 and 31 can be written as

$$\begin{bmatrix} M_1 & 0 & N_1 \\ 0 & M_2 & N_2 \\ N_1{}^T & N_2{}^T & 0 \end{bmatrix} \begin{bmatrix} \alpha_1 \\ \alpha_2 \\ \beta \end{bmatrix} = \begin{bmatrix} R_1 \\ R_2 \\ RR \end{bmatrix}, \quad \ldots\ldots(34)$$

where α_1, α_2, and β are the coefficients for the basis elements describing the x- and y-components of the velocity and the pressure, respectively. Eliminating α_1 and α_2 from Eq. 34 yields the linear system for β given by

$$(N_1{}^TM_1{}^{-1}N_1+N_2{}^TM_2{}^{-1}N_2)\beta$$
$$=-N_1{}^TM_1{}^{-1}R_1-N_2{}^TM_2{}^{-1}R_2+RR. \quad \ldots\ldots(35)$$

If N_x and N_y are the number of gridblocks in the x and y directions, respectively, the matrix N_1 is of size $2N_y\cdot(2N_x-1)\times 4N_xN_y$, and N_2 is of size $2N_x(2N_y-1)\times 4N_xN_y$. Although N_1 is not square, it has essentially a block diagonal form under a certain ordering of the gridblocks. N_2 can be made to have the same form by permitting the rows and corresponding columns. M_1 and M_2 are square, invertible matrices of size $2N_y(2N_x-1)\times 2N_y(2N_x-1)$ and $2N_x(2N_y-1)\times 2N_x(2N_y-1)$. The partitioned system is solved by preconditioned conjugate gradient procedures. Then, given β, α and α_2 are obtained by solving

$$M_1\alpha_1=R_1+N_1\beta \quad \ldots\ldots(36)$$

and

$$M_2\alpha_2=R_2+N_2\beta, \quad \ldots\ldots(37)$$

successively. Thus, although the full matrix in Eq. 34 is of size $[2N_y(2N_x-1)+2N_x(2N_y-1)+4N_xN_y]^2$, the system can be split up and solved using matrices which are no larger than matrix for pressure equation in a more standard formulation. For more details, see related Ref. 17 on computational aspects of mixed finite-element methods.

Finally, we briefly describe the interior penalty methods used in our codes. Let $\mathfrak{I}=\{T_1\ldots T_N\}$ be a partition of Ω into nonoverlapping rectangles, and let $E=E_0UE_\partial=\{e_1\ldots e_M\}\ U\{e_{M+1}\ldots e_Q\}$ be the collection of edges of the rectangle with $e_k\subset\Omega$ for $k\leqslant M$ and $e_k\subset\partial\Omega$ for $M<k\leqslant Q$. Let $|e|=$length (e). On each edge $e_k\epsilon E_0$, let the normal direction $n=n_k(x)$ be fixed at either (1, 0) or (0, 1). For $e_k\epsilon E_\partial$, let $n=n_k(x)=\nu$, the unit outward normal. Define

$$[f](x)=\lim_{\epsilon\downarrow 0}\{f[x-\epsilon n_k(x)]-f[x+\epsilon n_k(x)]\},\ x\epsilon e_k\epsilon E_0, \quad \ldots\ldots(38)$$

and

$$\{f\}(x)=\frac{1}{2}\lim_{\epsilon\downarrow 0}\{f[x-\epsilon n_k(x)]+f[x+\epsilon n_k(x)]\},$$
$$x\epsilon e_k\epsilon E_0. \quad \ldots\ldots(39)$$

For $x\epsilon e_k\epsilon E_\partial$, let $[f](x)=\{f\}(x)=f(x)$. Let $\sigma_j=\sigma_j(x,t)$ be continuous and nonnegative on each edge, and set, for $j=0, 1$:

$$J_j(f,g)=\sum_{e_k\epsilon E_0}|e_k|^{2j-1}\int_{e_k}\sigma_j\left[\frac{\partial^j f}{\partial n^j_k}\right]\left[\frac{\partial^j g}{\partial n^j_k}\right]ds. \quad \ldots\ldots(40)$$

TABLE 1—CONVERGENCE RATES—$a_1 = k/\mu \equiv 1$
Estimates: $\|u-U\| \leq K_1 h^{\alpha_1}$
$\|p-P\| \leq K_2 h^{\alpha_2}$

	Full Region Ω		Corners Removed	
	Standard	Singularities Removed	Standard	Singularities Removed
α_1	0.0	1.09	2.32	2.00
K_1	1.0	0.002	0.280	0.007
α_2	1.00	1.00	2.12	1.98
K_2	0.047	0.003	0.048	0.030

TABLE 2—CONVERGENCE RATES—VARIABLE $a \equiv k/\mu$
Estimates: $\|u-U\| \leq K_1 h^{\alpha_1}$

	Full Region Ω		Corners Removed	
	a_2	a_3	a_2	a_3
α_1	1.92	1.10	1.99	1.98
K_1	0.087	0.012	0.025	0.035

Let $(f,g)_T$ and $<f,g>_e$ indicate the inner products on $L^2(T)$ and $L^2(e)$, respectively. For a more complete motivation and explanation of this technique, see Refs. 6 through 9 and 18 and 19.

Using this notation, we can finally state our discrete-time mixed finite-element method. Find $(C;\ U;\ P)$:$\{0, t_1, ..T\} \rightarrow (M_h;\ V_h;\ W_h)$ satisfying Eq. 22, Eqs. 30 through 33, and

$$\left(\phi \frac{C^{n+1}-C^n}{\Delta t},\ z\right) - (EU^{n+1}EC^{n+1},\ \nabla z) + B(EU^{n+1};\ C^{n+1},\ z) - \sum_j Q_j(t)\hat{C}(x_j)z(x_j) = 0,\ z \epsilon M_h, \quad \ldots\ldots\ldots (41)$$

where x_j and $Q_j(t)$ are locations and flow rates at the wells, $Ef^{n+1} = 2f^n - f^{n-1}$, and the bilinear form B is defined by

$$B(s;f,g) = \sum_{T\epsilon} (D(s)\nabla f,\ \nabla g)_T + \sum_{j=0}^{1} J_j(f,g) - \sum_{e \epsilon E_0} \left[< D(s)\left\{\frac{\partial f}{\partial n_e}\right\},\ [g] >_e + < D(s)[f],\ \left\{\frac{\partial g}{\partial n_e}\right\} >_e \right]. \quad \ldots\ldots\ldots\ldots (42)$$

Numerical Results

The research codes developed to test our new methods have only recently been established and only preliminary testing has been completed. However, the initial results are very promising. Further research and testing of the codes is in progress.

Our first computation experiment was a study of asymptotic convergence rates for the Darcy velocity using several different choices of possibly variable permeabilities. The problem considered was a model of a two-well portion of a regular five-spot pattern. The computational domain Ω was normalized to the unit square, and Dirac delta functions with unit flow rates were used as well models at (0,0) and (1,1) for Eq. 2. Three choices of k/μ from Eq. 2 were tested:

$$a_1 \equiv \frac{k}{\mu}(x,y) \equiv 1,\ (x,y)\epsilon\Omega,$$

$$a_2 \equiv \frac{k}{\mu}(x,y) \equiv \begin{cases} 1, & x \leq 0.5, \\ 0.1, & x \geq 0.5, \end{cases}$$

$$a_3 \equiv \frac{k}{\mu}(x,y) = \frac{1}{1+10(x^2+y^2)},\ (x,y)\epsilon\Omega.$$

For each choice of k/μ given, the system (Eqs. 30 through 32) was solved on Ω with $h=0.25$, $h=0.0125$, $h=0.0625$, and $h=0.03125$, and convergence rates were

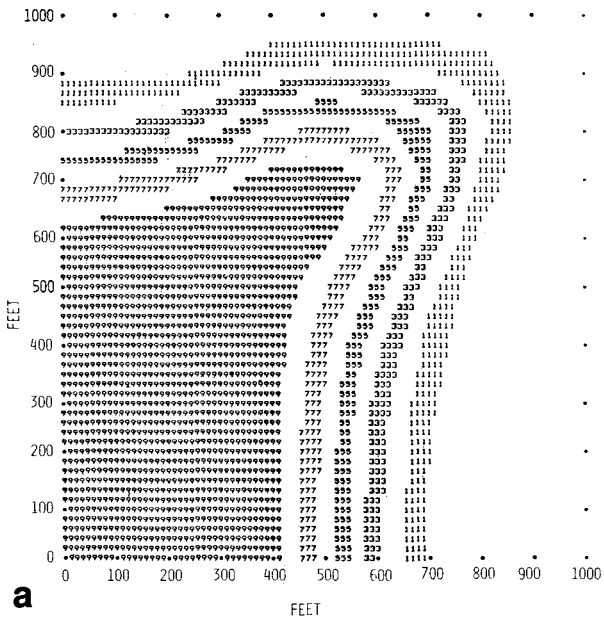

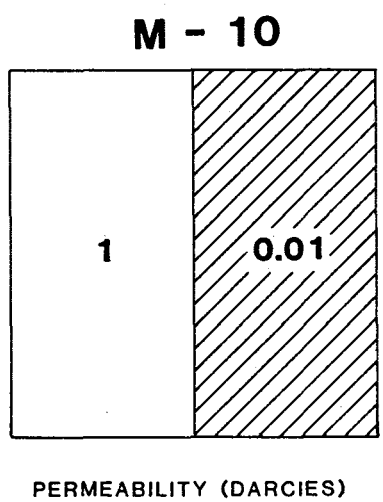

Fig. 1—Variable permeability. Contour map for concentration, 0.5 PV injected and 10 × 10 grid used for concentration, pressure, and velocities.

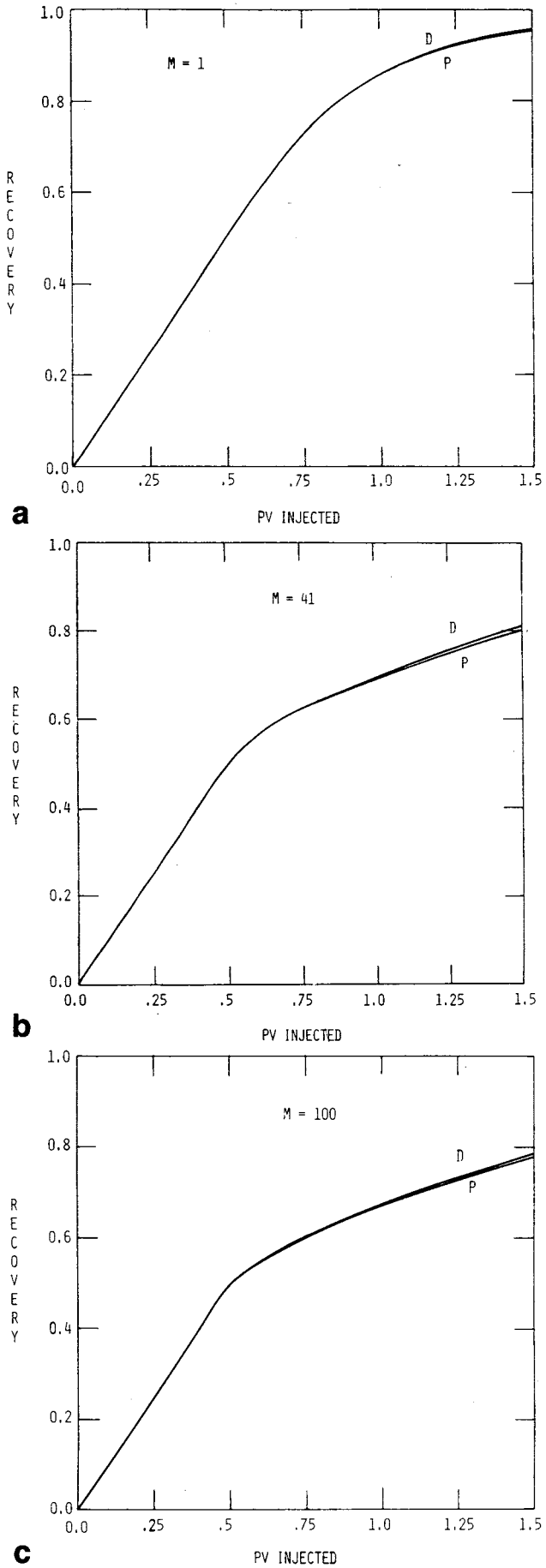

Fig. 2—Recovery curves for different grid orientations. "D" is diagonal (10 x 10) and "P" is parallel (14 x 14).

obtained for both the pressure, p, and the Darcy velocity, μ. The convergence rates were determined both for standard mixed methods and for methods where the singularities at the wells were removed as described in the preceding section. Since both p and u are smoother in regions away from the wells, we also determined convergence rates in "interior" regions with small corners of size 0.125 about each well removed. The convergence rates were measured in the standard L^2-norm on the indicated regions. Results of these convergence tests for the coefficient $k/\mu \equiv 1$ are presented in Table 1 for both the full domain Ω and for the interior domain with corners removed. The theoretically predicted convergence rates were obtained for both p and u, even though we were not in the asymptotic range of h. Similar experiments for the other choices of k/μ are given in Table 2. A more detailed convergence study of mixed method is presented in Ref. 17.

The matrices arising in Eq. 35 are not well conditioned for certain choices of rapidly changing coefficients k/μ. Thus in these cases, extensive iteration can be required to solve Eq. 35 unless either adequate scaling or preconditioning is applied or a good initial guess for the iteration is obtained. Various diagonal or incomplete Cholesky preconditioners have been used effectively[17] for mixed methods with varying coefficients. Further research in finding better preconditioners is in progress. In time-dependent problems, like the full miscible displacement system described in Eqs. 30 through 32 and Eq. 37, the solution pair (P,U) at the previous timestep serves as a very good initial guess for the conjugate gradient iteration[17] and the choice of preconditioner is not as important.

In all calculations with the full miscible displacement problem on the quarter five-spot problem, we set the resident viscosity to 1 cp [0.001 Pa·s], the viscosity exponent to 4, ϕ to 0.1, ϕd_m to 1 sq ft/D [0.093 m^2/d], and σ_1 to 250 and σ_2 to 0.5 from Eq. 36. We tested the miscible displacement problem, Eqs. 2 through 7, for several different choices of variable permeabilities.

By obtaining accurate velocities, we were able to run an experiment with

$$k[x,y] = \begin{cases} 1, & x \le 0.5,\ y \in [0, 1], \\ 0.01, & x > 0.5,\ y \in [0, 1]. \end{cases}$$

Previous codes described in the literature were not able to treat this case of rapidly changing permeability. A contour map describing the flow pattern for this experiment is given in Fig. 1.

We were also able to run our miscible displacement codes with different mobility ratios, varying from the simple case of $M=1$ to the very difficult case of $M=100$. The literature has not contained reports of satisfactory simulation of problems with $M=100$.

A problem encountered with finite-difference simulation of problems with high mobility ratios is a severe grid-orientation problem. We conducted grid-orientation studies with our methods and found only very minimal grid-orientation effects. The recovery curves presented in Fig. 2 and the contour maps presented in Fig. 3 demonstrate this lack of grid-orientation problems. We note that the computational results illustrated in Fig. 3

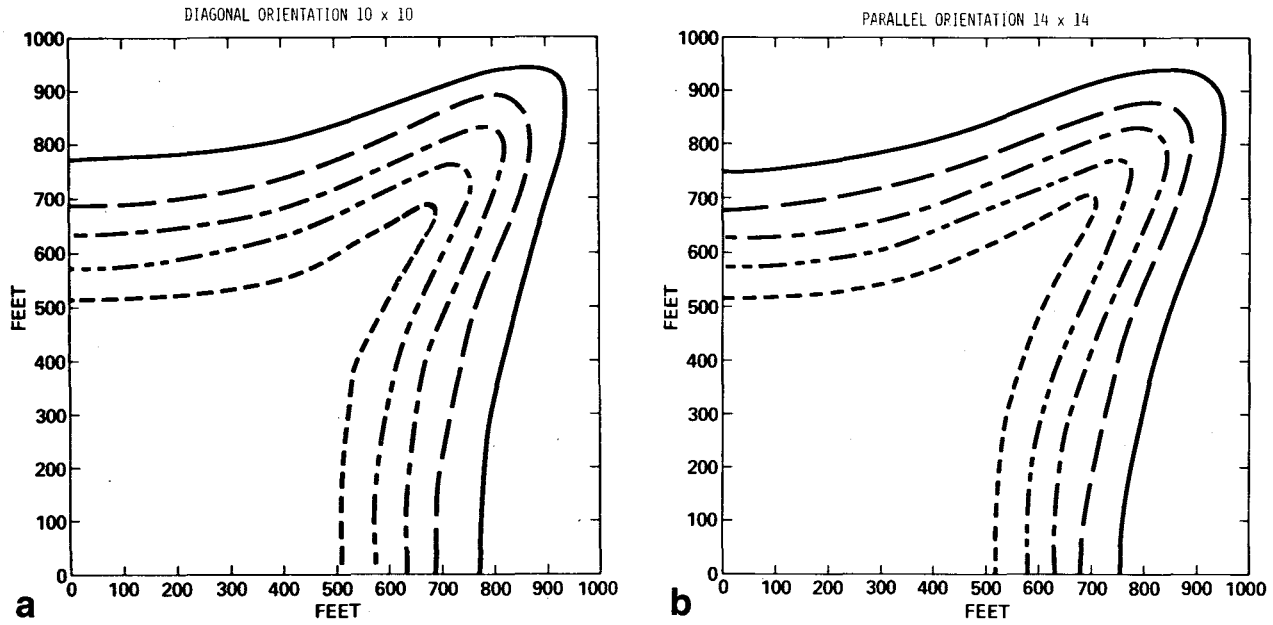

Fig. 3—Contour maps for concentration. $M=41$ and different grid orientations.

were very close and that the visual differences are due mainly to interpolation differences and drafting and not to grid orientation.

We were able to demonstrate the versatility of our research codes by running cases with tensor-diffusion, with lumping of the capacity matrix, and with various well placements. Two- and four-well sections of the five-spot flooding pattern were run to determine possible grid-orientation problems. We were also able to use a much coarser pressure grid than that used for concentration, in contrast to Darlow's work, because of our accurate velocity determination. We experimented with both a 5×5 pressure grid coupled with a 10×10 concentration grid and a 10×10 pressure grid coupled with a 20×20 concentration grid. We obtained the first satisfactory simulation to be reported using such coarse pressure grids. The number of unknowns in the mixed method with 10×10 pressure and 20×20 concentration grids is comparable with the number for the standard methods with 20×20 grids for both pressure and concentration. We also used less complicated quadrature rules in our codes than those used in Darlow's work with essentially no loss of accuracy and great computational savings.

In general, with the same choice of penalties, our codes produced slightly sharper fronts indicating less numerical dispersion than those presented earlier. Along with better accuracy near the fronts, we obtained slightly greater overshoot along the front, as expected. However, this slight overshoot dies out as the front moves across the reservoir and thus causes no stability problems. This overshoot indicates that insufficient parameters are being used to model a very sharp front and can be essentially eliminated by the use of adaptive local grid refinement along the front.

Conclusions

Mixed finite-element methods are potentially a very useful new numerical procedure for determining accurate Darcy velocities.

Mixed finite element methods for pressure approximation coupled with interior penalty Galerkin methods for concentration approximation demonstrate only minimal grid-orientation problems, even for very adverse mobility ratios of $M=41$ and $M=100$.

Accurate velocity approximation allowed simulation in regimes that were previously inaccessible: very coarse pressure grids, mobility ratios of the order $M=100$, and sharply changing permeability variations.

Accurate velocities aided simulation of sharp, moving fronts. Slight overshoot and undershoot cause no stability problems but merely reflect an inadequacy in the ability to realize sharp, moving fronts with coarse, fixed grids.

Nomenclature

B = bilinear form incorporating interior penalties
c = concentration of the invading fluid
$\hat{c}$ = inlet concentration for injection and resident concentration at projection wells
c_0 = initial concentration of the invading fluid
C = discrete approximation for concentration
d_ℓ = magnitude of longitudinal dispersion
d_m = magnitude of molecular dispersion
d_t = magnitude of transverse dispersion
D = diffusion-dispersion tensor
e = edges of rectangles in mesh
E = collection of edges of rectangles
E_0 = collection of interior edges of rectangles
E_∂ = collection of boundary edges of rectangles

h_c = spatial mesh for concentration equation
h_p = spatial mesh for pressure equation
J = time period
J_j = additions to bilinear form for penalties
k = permeability of the porous medium
M = mobility ratio
$M_j^m(\delta)$ = tensor product spaces of piecewise polynomials
N_j = logarithmic singularities at x_j
p = pressure of the total fluid
P_m = polynomials of degree at most m
P = discrete approximation for the pressure
q = total flow into or out of Ω
Q_j = flow rates at wells at x_j
t = independent time variable
T_i = non-overlapping rectangles
$\mathfrak{I}$ = union of T_i
u = Darcy velocity of total fluid
u_r = regular part of u
u_s = singular part of u
U = discrete approximation for u
U_r = discrete approximation for u_r
V,W = infinite dimensional function spaces
$V_h, \tilde{V}_h, W_h$ = finite dimensional function spaces
x,y = independent space variables
δ = mesh partition
ϵ = arbitrarily small positive parameter
μ = viscosity of the total fluid
ν = outward normal vector to $\partial\Omega$
σ_j = penalties on interior edges
ϕ = porosity of the porous medium
Ω = horizontal reservoir
$\partial\Omega$ = boundary of reservoir

Acknowledgments

We thank Exxon Production Research Co. and Mobil R&D Corp. for permission to publish this paper. The authors also thank Jim Douglas Jr. for several valuable suggestions.

We thank Douglas Arnold for suggesting the source-and-sink subtraction treatment described.

References

1. Peaceman, D.W.: *Fundamentals of Numerical Reservoir Simulation,* Elsevier Publishing Co., New York City (1977).
2. Settari, A., Price, H.S., and Dupont, T.: "Development and Application of Variational Methods for Simulation of Miscible Displacement in Porous Media," *Soc. Pet. Eng. J.* (June 1977) 228–46.
3. Ewing, R.E. and Wheeler, M.F.: "Galerkin Methods for Miscible Displacement Problems in Porous Media," SIAM *J. Numer. Anal.*(1980) **17**, 351–65.
4. Peaceman, D.W.: "Improved Treatment of Dispersion in Numerical Calculation of Multidimensional Miscible Displacement," *Soc. Pet. Eng. J.* (1966) 213–16.
5. Douglas, J. Jr., Ewing, R.E., and Wheeler, M.F.: "The Approximation of the Pressure by a Mixed Method in the Simulation of Miscible Displacement" *RAIRO Anal. Numer.* (1983) **17**, 17–33.
6. Douglas J. Jr.: "The Numerical Solution of Miscible Displacement in Porous Media," *Computational Methods in Nonlinear Mechanics,* J.T. Oden (ed.), North Holland Publishing Co., New York City (1980) 225–38.
7. Wheeler, M.F. and Darlow, B.L.: "Interior Penalty Galerkin Methods for Miscible Displacement Problems in Porous Media," *Computational Methods in Nonlinear Mechanics,* J.T. Oden (ed.), North Holland Publishing Co., New York City (1980) 485–506.
8. Wheeler, M.F.: "An Elliptic Collocation Finite Element Method with Interior Penalties," *SIAM J. Numer. Anal.* (1978) **15**, 152–61.
9. Darlow, B.L.: "A Penalty-Galerkin Method for Solving the Miscible Displacement Problem," PhD dissertation, Rice U., Houston (1980).
10. Douglas J. Jr.: "Simulation of Miscible Displacement in Porous Media by a Modified Method of Characteristic Procedure," *Numerical Analysis,* Dundee 1981, Lecture Notes in Mathematics 912, Springer-Verlag, Heidelberg (1982).
11. Raviart, P.A. and Thomas, J.M.: "A Mixed Finite Element Method for Second Order Elliptic Problems," *Mathematical Aspects of the Finite Element Method,* Rome 1975, Lecture Notes in Mathematics, Springer-Verlag, Heidelberg (1977).
12. Brezzi, F.: "On the Existence, Uniqueness and Approximation of Saddle-Point Problems Arising from Lagrangian Multipliers," *RAIRO Anal. Numer.* (1974) **2**, 129–51.
13. Falk, R.S. and Osborn, J.E.: "Error Estimates for Mixed Methods," *RAIRO Anal. Numer.* (1980) **14**, 249–77.
14. Ewing, R.E. and Wheeler, M.F.: "Galerkin Methods for Miscible Displacement Problems with Point Sources and Sinks-Unit Mobility Ratio Case," *Proc.,* Special Year in Numerical Analysis, U. of Maryland, College Park (1981) (to appear).
15. Ewing, R.E. and Russell, T.F.: "Efficient Time-Stepping Procedures for Miscible Displacement Problems in Porous Media," *SIAM J. Numer. Anal.* (1982) **19**, (to appear).
16. Douglas, J. Jr., Ewing, R.E., and Wheeler, M.F.: "A Time-Discretization Procedure for a Mixed Finite Element Approximation of Miscible Displacement in Porous Medium," *RAIRO Anal. Numer.* (1983) 249–65.
17. Ewing, R.E. and Wheeler, M.F.: "Computational Aspects of Mixed Finite Element Methods," *Numerical Methods for Scientific Computing,* R.S. Stepleman (ed.), North Holland Publishing Co., New York City (1983).
18. Douglas, J. Jr. and Dupont, T.: "Interior Penalty Procedures for Elliptic and Parabolic Galerkin Methods," *Computing Methods in Applied Science,* Lecture Notes in Physics 58, Springer-Verlag, Heidelberg (1976).
19. Arnold, D.N.: "An Interior Penalty Finite Element Method with Discontinuous Elements," MS thesis, U. of Chicago (1979).
20. Yanosik, J.L. and McCracken, T.A.: "A Nine-Point Finite-Difference Reservoir Simulator for Realistic Prediction of Unfavorable Mobility Ratio Displacement," paper SPE 5734 presented at the 1976 SPE Reservoir Simulation Symposium, Los Angeles, Feb. 19–20.

SI Metric Conversion Factor

ft × 3.048* E−01 = m

*Conversion factor is exact.

SPEJ

Original manuscript received in the Society of Petroleum Engineers office Feb. 3, 1982. Paper accepted for publication Nov. 22, 1982. Revised manuscript received Aug. 19, 1983. Paper (SPE 10501) first presented at the 1982 SPE Reservoir Simulation Symposium held in New Orleans Jan. 31–Feb. 3.